

The spin rates of O stars in WR + O binaries. I. Motivation, methodology and first results from SALT

Michael M. Shara^{1*}, Steven M. Crawford², Dany Vanbeveren³,
Anthony F. J. Moffat⁴, David Zurek¹ and Lisa Crause²

¹*Department of Astrophysics, American Museum of Natural History, Central Park West at 79th Street, New York, NY 10024, USA*

²*South African Astronomical Observatory, P.O. Box 9, Observatory 7935, Cape Town, South Africa*

³*Astrophysical Institute, Vrije Universiteit Brussel, Pleinlaan 2, 1050, Brussels, Belgium*

⁴*Département de Physique, Université de Montréal, CP 6128 Succ. C-V, Montréal, QC H3C 3J7, Canada*

Accepted Received

ABSTRACT

The black holes (BH) in merging BH-BH binaries are likely progeny of binary O stars. Their properties, including their spins, will be strongly influenced by the evolution of their progenitor O stars. The remarkable observation that many single O stars spin very rapidly can be explained if they accreted angular momentum from a mass-transferring, O-type or Wolf-Rayet companion before that star blew up as a supernova. To test this prediction, we have measured the spin rates of eight O stars in Wolf-Rayet (WR) + O binaries, increasing the total sample size of such O stars' measured spins from two to ten. Polarimetric and other determinations of these systems' $\sin i$ allow us to determine an average equatorial rotation velocity from HeI (HeII) lines of $v_e = 348$ (173) km/s for these O stars, with individual star's v_e from HeI (HeII) lines ranging from 482 (237) to 290 (91) km/s. We argue that the $\sim 100\%$ difference between HeI and HeII speeds is due to gravity darkening. Super-synchronous spins, now observed in all 10 O stars in WR + O binaries where it has been measured, are strong observational evidence that Roche lobe overflow mass transfer from a WR progenitor companion has played a critical role in the evolution of WR+OB binaries. While theory predicts that this mass transfer rapidly spins-up the O-type mass gainer to a nearly break-up rotational velocity $v_e \sim 530$ km/s, the observed average v_e of the O-type stars in our sample is 65% that speed. This demonstrates that, even over the relatively short WR-phase timescale, tidal and/or other effects causing rotational spin-down must be efficient. A challenge to tidal synchronization theory is that the two longest-period binaries in our sample (with periods of 29.7 and 78.5 days) unexpectedly display super-synchronous rotation.

Key words: surveys – binaries: massive – stars: Wolf-Rayet – stars:black holes

1 INTRODUCTION

When massive stars rotate sufficiently rapidly (i.e. with equatorial velocities > 200 - 300 km/s) their rotation fundamentally influences their evolution (Maeder & Meynet 2000; Heger & Langer 2000; Hirschi, Meynet, & Maeder 2004; Yoon & Langer 2005; Brott et al. 2011; Ekström et al. 2012). Rapid rotation may critically affect the final collapse of a massive star, leading to ultra-luminous supernovae and long-duration gamma-ray bursts (Woosley & Heger 2006; Georgy et al. 2009). Many O-stars and their progeny, the

Wolf-Rayet (WR) stars, are found in binary systems. Merging binary black holes (Abbott et al. 2016) that were generated in WR + O binaries may have spins determined by the evolution of the binary components. Those spins will be measurable with Advanced LIGO and Virgo (Pürrer, Hannam, & Ohme 2016).

The theoretically-predicted importance of rotation has motivated several observational studies to measure the distribution of rotational velocities of massive stars. Galactic massive stars' rotation is studied in Penny (1996); Howarth et al. (1997); Vanbeveren et al. (1998a), while the VLT Tarantula survey examined similar stars in the LMC (Dufton et al. 2013; Ramírez-Agudelo et al. 2013). All of

* E-mail: mshara@amnh.org

these studies reached a similar conclusion: the distribution for both the early B-type stars and O-type stars is bimodal. The majority of these stars are relatively slow rotators with an average equatorial velocity $v_e \sim 100$ km/s, while a smaller, but significant fraction of them are rapid rotators with $v_e > 200$ km/s, reaching up to 500-600 km/s. The early Be-type stars obviously belong to the early B-type high velocity tail.

The Geneva team (Ekström et al. (2012) and references therein) attempted to determine the average equatorial velocity $\langle v_e \rangle$ of massive single stars at birth under the assumption that the overall bimodal distribution, noted above, is the norm for massive single stars in general. They concluded that $\langle v_e \rangle \sim 300$ km/s. This has been the value used in most of the massive single star evolutionary calculations published by the Geneva team in the last 15 years.

1.1 Binaries

However, it was argued decades ago that a significant fraction of all massive stars are close binary components (for extended reviews see van den Heuvel (1993); Vanbeveren (1998b); Vanbeveren et al. (1998a)), and that a significant fraction of the rapid rotators may have a binary origin. Since 1998 several extensive observational campaigns have confirmed that most (and perhaps all) massive stars are born in close binaries (Mason et al. 1998, 2009; Sana & Evans 2011; Sana et al. 2013). The suggestion that “many rapid rotators have a binary origin” has become more and more plausible. A theoretical study by de Mink et al. (2013), which used overall population synthesis tools and included binaries, successfully reproduces the observed distribution of rotation rates of massive stars.

Vanbeveren, De Loore, & Van Rensbergen (1998c) posed the questions of whether the WR components in WR+OB binaries formed by stellar wind mass loss, or by binary mass loss processes (Roche Lobe Overflow -RLOF - or Common Envelope -CE), and if RLOF happened in WR+OB binary progenitors, was it accompanied by mass transfer and mass accretion? When primaries exceed ~ 40 - $50 M_\odot$ they may lose a significant fraction of their initial masses via stellar winds, greatly increasing the binary period. The existence of WR + O binaries with periods of days can only come about via RLOF or CE phases. The progenitor of a WR+OB binary, where the OB star has luminosity class V, or where the O component is an early O-type star, most likely underwent RLOF and mass transfer, causing the rejuvenation of the gainer (Vanbeveren, De Loore, & Van Rensbergen 1998c).

Rapid rotation in close binaries can arise during Roche lobe overflow (RLOF) when mass lost by the mass donor is accreted by the mass gainer (Vanbeveren 1998b). Mass accretion is accompanied by angular momentum accretion, hence, in this scenario, the mass gainer spins up and becomes a rapid rotator (Packet 1981). When the mass donor ends its life with an asymmetric supernova explosion, the binary may be disrupted. This binary supernova scenario successfully predicts that the escaped component (the mass gainer) will be a rapidly rotating single runaway star (defined as a star with peculiar space velocities > 30 km/s (Blaauw 1961)). Most of the known massive runaway stars are rapid rotators, with ζ Pup being the prototype (Vanbeveren 2012). ζ Pup

displays spectral class O4 I(n)fp (Sota et al. 2014). While uncertainties in its distance (Maíz Apellániz, Alfaro, & Sota 2008; Schilbach & Röser 2008) translate directly into uncertainties in its radius ($14 - 26 R_\odot$) and mass ($22 - 56 M_\odot$), and hence its critical rotation speed ($550 - 640$ km/s), its observed $v_e \sin(i)$ of 220 km/s (Vanbeveren 2012) is $\sim 35 - 40\%$ of its critical rotation speed.

1.2 Testing a prediction of RLOF

The motivation of this and subsequent papers is to test the prediction of RLOF-driven spin-up in massive, Wolf-Rayet (WR) + O binary stars (Petrovic, Langer, & van der Hucht 2005). Most classical Wolf-Rayet (WR) stars are core helium burning objects that have lost their hydrogen-rich layers. This has occurred via stellar wind mass loss, if the WR star is a single star or in a wide, non-interacting binary, and/or by RLOF when the WR star is a close-binary component. O-type companions to WR stars that are spinning super-synchronously (with $v_e \sin i$ typically > 100 km/s in binaries with periods shorter than about 10 days) are strongly indicative of RLOF mass and angular momentum accretion (Vanbeveren 1998b). An example is WR 127, which contains a $23.9 M_\odot$ O V star and a $13.4 M_\odot$ WR star in a 9.555 day orbit that is inclined at 55.3 degrees to the line-of-sight (de La Chevrotière, Moffat, & Chené 2011). The Martins, Schaerer, & Hillier (2005) calibration for O-star radii (their table 1) yields $8.11 R_\odot$ as the radius of the O star in WR 127. If the O star were rotating synchronously it would display a $v_e \sin i$ of 36 km/s. The observed value is ~ 250 km/s (Massey 1981), which is highly super-synchronous.

A comprehensive study of the rotational velocities of the O-type components of WR+O binaries would be a valuable test of the idea that many rapid rotators have a binary origin, and have undergone RLOF mass transfer. A literature search reveals that the $v_e \sin i$ value of the O-type components of WR + O binaries have been measured for only two systems, and estimated for one more. In one carefully measured case (V444 Cyg = WR139 (Marchenko, Moffat, & Koenigsberger 1994)), the O-type component is observed to be a rapid rotator, with $v_e \sin i = 215 \pm 13$ km/s. In the second measured case (the brightest and nearest WR+O binary in the sky = WR 11 (Baade, Schmutz, & van Kerkwijk 1990)), the O7.5 giant displays $v_e \sin i = 220 \pm 20$ km/s. For HD 186943 = WR127 (Massey 1981), the widths of the O stars’ absorption lines were estimated to correspond to $v_e \sin i \sim 200 - 250$ km/s. $v_e \sin i = 200 - 250$ km/s is significantly faster than the v_e corresponding to binary synchronicity in all three systems, and suggestive, though not conclusive evidence that RLOF has been important in the systems’ evolution. Despite these encouraging early works, a systematic, quantitative study of O-star spins in WR + O binaries, both from a theoretical and an observational point of view, has not yet been carried out.

The test of whether O companions in WR+O binaries are spun up by binary accretion can best be accomplished by measuring the observational line width parameter $v \sin i$ of the O component from line broadening of helium lines (Ramírez-Agudelo et al. 2013, 2015). Once this is available then one wants, ideally, to extract v_e , the equatorial rota-

tion speed of the star. A binary's $\sin i$ may be obtained from polarimetry, photospheric or atmospheric eclipses, colliding-wind analysis, by assuming a mass for the O star from its spectral type if not otherwise known, or from visual binary orbits (Moffat 2008). If one assumes alignment of the spin axes of the binary components with the binary axis, then $\sin i$ is also known for the O-star axis. However, this may not always be a good assumption (e.g. Villar-Sbaffi et al. (2005, 2006) for CQ Cep and CX Cep, two very-short period Galactic WR+O binaries, where the orbital and spin axes are misaligned). Therefore, one needs a large number of systems from which one can extract statistical information from $v_e \sin i$ to deduce $\langle v_e \rangle$. This is precisely the methodology adopted in studies of rotation speeds of single field O stars (Ramírez-Agudelo et al. 2013), and in studies of O + O star binaries (Ramírez-Agudelo et al. 2015). In this study we have succeeded in measuring the $v_e \sin i$ of eight O stars in WR + O binaries, thereby raising the sample size with well-measured spin rates from two to ten.

In Section 2 we describe the data and their reductions. The high resolution spectra of the helium lines of the O stars we study are presented in Section 3, as well as these stars' derived rotation rates. In section 4 we discuss the implications of our results for the overall evolution of rotational velocities in massive binaries, and we briefly summarize our results in Section 5.

2 OBSERVATIONS AND DATA REDUCTIONS

2.1 Observations

Observations¹ of the target stars were obtained with the High Resolution Spectrograph (Crause et al. 2014) (HRS) of the Southern African Large Telescope (SALT). The HRS is a dual beam, fiber-fed echelle spectrograph. It was used in low resolution mode with a 2.23" arcsec diameter fiber to provide a spectrum in the blue arm over the spectral range of 3700–5500 Å. All of the spectra have a resolving power $R \sim 12,700$ and signal-to-noise ratio S/N per pixel > 150 , designed to counterbalance the diluting effects of the accompanying WR spectrum. The observations from the blue arm were read out by a single amplifier with 1×1 binning. All observations of our target stars were obtained between May and June 2015 with most of the objects observed twice, i.e. once on each of two separate nights. During this time, a single ThAr arc and spectral flats were obtained in this mode for the purposes of calibration. In addition, observations of τ Sco were obtained on 7 August 2015 to provide a measurement of a source with a known, low value for $v_e \sin i$. Basic CCD reductions including bias subtractions, gain corrections, and flat fielding were handled by the `ccdproc` package (Crawford 2015).

Spectroscopic reductions of the data were carried out using the `pyhrs` package (Crawford 2015). The software created an order frame from a flat field image that assigned each pixel in the image to a specific order. Prior to extracting, each order was corrected for spatial and spectral curvature. A second order polynomial was fit to the overall shape of the

order, which was then removed. In addition, each row of the order was corrected for a small offset in the vertical direction between each of the rows of the order. This offset was well below the size of the resolution element for the low resolution mode. To calculate the wavelength solution, a spectrum was extracted by summing the rows in the order. The resultant spectrum was then passed to the `specidentify` task in the PySALT reduction package (Crawford et al 2010) for wavelength identification and calculation of the wavelength solution. Next, the target spectrum was extracted from our observations. The extraction of the order was performed as described with the final spectrum being a result of a flux-weighted co-addition of all of the illuminated rows in the order and the wavelength derived from the solution calculated for that order. As a minimum of two exposures were taken for each observation, the final step combined the extracted spectra from these two exposures to produce the final spectrum for each star. HRS does have a sky and target fiber, but as the target fiber only was used in our analysis, all steps were only performed on the target fiber.

2.2 Resolution of the SALT HRS

The expected FWHM for an unresolved line at $\lambda = 4750$ Å is ~ 0.37 Å, corresponding to a resolving power $R \sim 12,700$, based on the predicted performance of the HRS spectrograph (Crause et al. (2014), Table 2). This corresponds to a velocity resolution of 24 km/s. As this is one of the first papers reporting results with the newly commissioned SALT HRS, and measured line widths are central to our analyses, we have measured the FWHM of several arc lines close to the wavelengths of the strongest HeI and HeII O stars' lines. An example is given in Figure 1, where an arc line at $\lambda 4541$ displays a FWHM of 0.30 ± 0.02 Å, better than the predicted value.

As a further test of our methodology and the resolving power of HRS, we observed the bright B0.2V star τ Sco = HD 149438. The most recently measured $v_e \sin i$ of τ Sco = 4 km/s (Nieva & Przybilla 2012). This extremely low value of $v_e \sin i$ demonstrates that the effects of thermal Doppler broadening, Stark effect, and micro and macro-turbulence are very small in a star of spectral type nearly identical to that of our coolest observed O star. Of course, this is no guarantee that the O stars' He lines in the O + WR binaries that we study below do not undergo line broadening from one or more of the above mechanisms. Indeed, Sundqvist et al. (2013) describe two magnetic O stars with rotation periods longer than one year, and hence with $v_e \sin i \leq 1$ km/s, whose line widths imply $v_e \sin i \sim 40$ –50 km/s. They note that the severe overestimates based on line widths alone are most likely caused by an insufficient treatment of microturbulence and macroturbulence, and that these broadening mechanisms can dominate line profiles in stars with $v_e \sin i$ up to ~ 40 –50 km/s.

Due to structure in the outer profiles of each line preventing the lines from being well fit by a single Gaussian, we measured the FWHM directly for each of the HeI $\lambda 4387$, $\lambda 4713$, and $\lambda 4922$ lines in τ Sco (see Figure 2). The average $v_e \sin i$ from the three lines, using the same methodology described below for our program stars, was 24 ± 3 km/s. This observed value is, of course, instrumental, as the HRS low resolution mode broadens the very narrow lines of τ Sco

¹ Observations were taken under SALT Proposal Code: 2015-1-SCI-064.

to its resolution limit. All of our program stars, discussed below, display FWHM of He absorption lines that are 10 to 20 times larger than the resolution limit of SALT's HRS low resolution mode, corresponding to $v. \sin i$ (for HeI lines) that always exceed 200 km/s. Simulations show that the blending of the satellite lines seen in Figure 2 with the 4922 line due to spin speeds in excess of 150 km/s *and* micro- or macro-turbulence of 50 km/s cause us to overestimate $v. \sin i$ by less than 15% in all cases.

2.3 Line Analysis

To determine the value for $v. \sin i$ for the stars in our sample, we followed the process as outlined in detail by Ramírez-Agudelo et al. (2013) and Ramírez-Agudelo et al. (2015). This involved measuring the broadening of these stars' HeI and HeII lines via the full width at half maximum (FWHM). To measure the FWHM of the lines in our stars, we used the **astropy** modeling software (Astropy Collaboration et al. 2013) to fit Gaussian curves to the HeI $\lambda 4922$ and/or HeII $\lambda 4541$ lines (WR30, WR47, and WR79 only exhibited the HeII $\lambda 4541$ line). Prior to fitting the Gaussian curve, a low-order polynomial was fit to the area outside of the line and divided through to normalize the continuum. Errors for the fits were calculated through a bootstrap Monte Carlo method of resampling the spectra using the flux errors and repeating the fit. From the fits, we determined the FWHM for each of the lines and then converted the values for the FWHM to velocities based on the relationships in Table 1 of Ramírez-Agudelo et al. (2015).

Finally, we directly measured the FWHM of the He I $\lambda 4471$ line for WR 127 from Figure 8 of de La Chevrotière, Moffat, & Chené (2011).

3 RESULTS: THE O STARS' HELIUM LINES

The fit to each of the continuum-divided absorption lines of HeI and HeII in each of our eight WR + O binaries is presented in Figures 3 through 10.

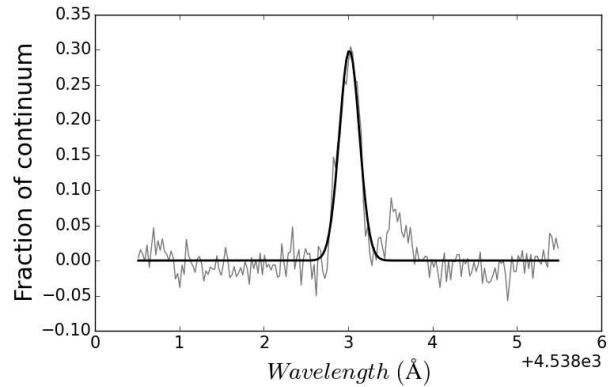


Figure 1. A SALT High Resolution Spectrograph arc line close to the HeII 4541 line. The line's FWHM is $0.30 \pm 0.02 \text{ \AA}$. The data points are in light gray while the model fit is the solid black curve in this and all following figures.

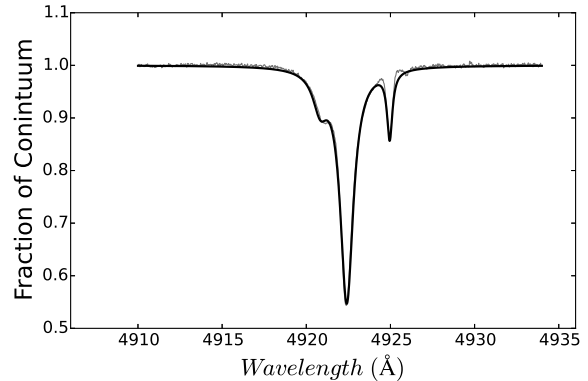


Figure 2. The HeI 4922 absorption line of the slowly rotating star τ Sco on 07 Aug 2015.

In Table 1, we report our measured HeI and HeII FWHM and velocities for each of eight O stars in WR + O binaries, for τ Sco, and for WR 127 from Figure 8 of de La Chevrotière, Moffat, & Chené (2011). HeI absorption lines were detected in five O stars by SALT (WR 21, WR 31, WR 42, WR 97 and WR 113), and in WR 127 by de La Chevrotière, Moffat, & Chené (2011), while the HeII $\lambda 4541$ line was detected in these same five stars as well as in WR 30, WR 47 and WR 79.

The smallest FWHM measured in any of the target stars in our sample is $3.62 \pm 0.04 \text{ \AA}$ (for the HeII $\lambda 4541$ line) which corresponds to a $v. \sin i$ of 89 ± 11 km/s for WR 21. The largest FWHM measured is $7.25 \pm 0.05 \text{ \AA}$ (for the HeI $\lambda 4922$ line), which corresponded to a $v. \sin i$ of 315 ± 21 km/s for WR 42. For each star with more than one measurement of $v. \sin i$, (because of multiple epochs and/or more than one line measured), we adopt an average value from all its measurements. The average $v. \sin i$ for our sample of eight O stars with measured HeII lines is 137 km/s. The average $v. \sin i$ for our sample of six O stars with measured HeI lines is 268 km/s, which is nearly twice as large as the HeII lines' $v. \sin i$. We return to this large difference below.

These data can now be combined with orbital inclinations gleaned from the literature. In table 2 we present these data, which yields (by far) the largest ensemble of rotational

Table 1. Measured FWHM and $v_e \sin i$ of τ Sco and O stars in O+WR star binaries

Object	Observed	HeI $\lambda 4471, 4922$ FWHM (\AA)	HeI $v_e \sin i$ (km/s)	He II $\lambda 4541$ FWHM (\AA)	HeII $\lambda 4541$ $v_e \sin i$ (km/s)
WR21	2015-05-08	5.96 ± 0.23	246 ± 20	3.62 ± 0.04	89 ± 11
WR21	2015-05-24	5.24 ± 0.17	209 ± 16	4.31 ± 0.03	120 ± 16
WR30	2015-05-08	5.46 ± 0.23	178 ± 27
WR31	2015-05-08	5.37 ± 0.05	216 ± 15	5.40 ± 0.05	176 ± 23
WR42	2015-05-08	7.25 ± 0.05	315 ± 21	4.09 ± 0.04	109 ± 14
WR42	2015-05-21	4.36 ± 0.05	122 ± 16
WR47	2015-05-21	3.65 ± 0.13	90 ± 13
WR47	2015-05-22	3.54 ± 0.06	86 ± 11
WR79	2015-05-08	4.34 ± 0.03	121 ± 16
WR79	2015-05-21	4.35 ± 0.04	121 ± 16
WR79	2015-05-22	4.46 ± 0.06	127 ± 17
WR97	2015-05-12	5.66 ± 0.12	230 ± 17	4.65 ± 0.03	136 ± 18
WR97	2015-06-13	6.11 ± 0.14	254 ± 18	4.96 ± 0.05	152 ± 20
WR113	2015-05-24	7.16 ± 0.13	310 ± 22	5.26 ± 0.07	168 ± 22
WR113	2015-06-07	7.14 ± 0.14	309 ± 22	5.35 ± 0.06	172 ± 23
WR127	2004 June-July	7.0 ± 0.5	300 ± 30
τ Sco	2015-05-08	0.30 ± 0.06	24 ± 3

velocities of O stars in WR + O binaries yet assembled. The errors in derived v_e are dominated by the uncertainties in orbital inclinations. In the final column of Table 2 we also list the synchronous rotation speeds and critical rotation speeds of the O-stars in each binary, using the already-measured masses and the spectral type-radius calibration of Martins, Schaerer, & Hillier (2005). A key result of this paper is that the average equatorial rotational velocity of six O stars, measured from HeI lines, is a highly super-synchronous 348 km/s. The average equatorial rotational velocity of eight O stars, measured from HeII lines, is 173 km/s, which is still significantly super-synchronous.

4 OBSERVATIONS CONFRONT THEORY

4.1 HeI versus HeII lines' rotation speeds: oblate O stars

Ramírez-Agudelo et al. (2013) have noted that values of $v_e \sin i$ for *single* O stars measured from HeII absorption lines are systematically lower than those measured from HeI lines by 25% (see their Figure 10). They suggested that gravity darkening was responsible for this systematic difference. Rapid rotation produces equatorial centrifugal support of stars, hence oblateness and lower surface gravity at the equator, which is thus cooler and darker. Photospheric regions closer to the poles (equators) should then contribute more to the formation of He II (He I) lines. Projected rotational velocities derived from He II lines should thus be lower than those from HeI lines, as observed in Figure 10 of Ramírez-Agudelo et al. (2013).

von Zeipel's theorem (von Zeipel 1924) states that the radiative flux in a uniformly rotating star is proportional to the local effective gravity. Spectrographic observations, constrained by interferometric measurements of rapidly rotating stars show convincingly that latitudinal large temperature differences exist in the rapidly rotating stars Alpha Leo, Alpha Aquila and Achernar (McAlister et al. 2005; Monnier et al. 2007; Domiciano de Souza et al. 2014).

In particular, Alpha Leo displays equatorial (polar) temperatures of 10,314 K (15,400 K) (McAlister et al. 2005). Achernar similarly displays equatorial (polar) temperatures of 12,673 K (17,124 K) (Domiciano de Souza et al. 2014). A recent review of the observations of these and other rapidly spinning stars is given by Claret (2016). These observations demonstrate conclusively that the polar temperatures of rapidly rotating stars can be 50% hotter than their equatorial temperatures.

Modern theoretical studies of gravity darkening (Espinosa Lara & Rieutord 2011; Claret 2016) conclude that von Zeipel's theorem is only applicable to slowly rotating stars. Espinosa Lara & Rieutord (2011) demonstrate that latitudinal variations in the effective temperature of a rapidly rotating star depend on the ratio of the equatorial velocity to the Keplerian velocity. Their model demonstrates good agreement with the above-noted observations of Alpha Leo and Alpha Aquila. Claret (2016) obtains good agreement with observed gravity darkening indices for six rapidly rotating stars by considering optical depth effects in these stars' atmospheres.

While our primary goal in undertaking this observational study was to determine whether RLOF-induced, super-synchronous rotation is seen in the O stars in WR + O binaries, an unexpected bonus has emerged. *Our observations indicate that not only are the O stars rotating super-synchronously, they also display large variations of effective temperature with latitude, suggesting that they may be oblate.* Since we are interested in the speeds of rotation at the equators of our O stars, it is clear that the velocities we derive from the HeI lines, and *not* those of the HeII lines are the speeds to use.

4.2 Tides and RLOF

Mass transfer during RLOF, wherein some of the mass lost by a donor star is accreted by its companion, is accompanied by angular momentum transfer, which forces the mass gainer to spin-up. It was demonstrated by Packet (1981)

Table 2. WR + O star binaries' properties

System	Spectral Types	Period(d)	$M(\text{WR}+\text{O})\sin^3 i (M_\odot)$	$i(\text{deg})$	HeI $v_e(\text{km/s})$	HeII $v_e(\text{km/s})$	O-star $v(\text{sync})/v(\text{crit})(\text{km/s})$
WR 21	WN5o + O4-6	8.3	8.4 ± 16.3	48 – 62	278 – 331	115 – 138	70/528
WR 30	WC6 + O6-8	18.8	15.4 ± 31.9	78 – 90	...	178 – 182	25/818
WR 31	WN4o + O8 V	4.8	2.7 ± 6.3	40 – 62	244 – 336	199 – 274	89/382
WR 42	WC7 + O7 V	7.9	3.7 ± 6.2	38 – 44	453 – 511	157 – 177	66/361
WR 47	WN6o + O5 V	6.2	40 ± 47	67 – 90	...	88 – 96	93/897
WR 79	WC7 + O5-8	8.9	1.8 ± 4.9	34 – 45	...	174 – 220	53/321
WR 97	WN5b + O7	12.6	2.3 ± 4.1	31 – 85	243 – 470	146 – 279	39/293
WR 113	WC8d + O8-9 IV	29.7	10.6 ± 22.3	70 – 90	310 – 330	170 – 181	19/623
WR 127	WN5o + O8.5 V	9.6	13.4 ± 23.9	55 – 90	300 – 366	...	42/697
WR 11	WC8 + O7.5 III	78.5	6.8 ± 21.6	63	220	...	9/545
WR 139	WN5o + O6 III-V	4.2	8.8 ± 26.3	78.7	215	...	151/640

Spectral Types from Crowther (2015) and de La Chevrotière, Moffat, & Chené (2011)); Mass functions and inclinations from Lamontagne et al. (1996);

$v_e \sin i$ references: This paper, except for WR 127 (de La Chevrotière, Moffat, & Chené 2011), WR 11 (Baade, Schmutz, & van Kerkwijk 1990), and WR 139 (Marchenko, Moffat, & Koenigsberger 1994)

that when the RLOF-process in a case B binary² is quasi-conservative, then soon after the onset of this process the mass gainer is spun up to its critical Keplerian speed. Since the observed rotational velocity of the O-type companions in all 10 of the WR binaries in which it has now been measured is super-synchronous, it is tempting to conclude that mass transfer and spin-up have played important roles during the progenitor evolution.

To further explore this scenario we assume that, very soon after the RLOF process began in the binaries we now observe, the O-type mass gainer was rotating critically. This corresponds to Keplerian rotation speeds of ~ 530 km/s. The average rotation speed of six O-type companions with HeI lines in our observed binary sample is 348 km/s, close to 65% of the Keplerian value. The evolutionary timescale of a WR star is typically of the order of a few hundred thousand years. Thus the 348 km/s observed rotation speed means that, even over this short timescale, tidal interactions must be efficient, able to cause significant spin-down of the O-type companions.

We conclude by noting that the two longest period WR binaries in our sample (WR 113 at $P = 29.7$ d and WR 11 with $P = 78.5$ d) each have an O-type companion that is rotating super-synchronously, but with speeds that are significantly below critical. We are unaware of a tidal-synchronization theory (e.g., Hut (1981); Tassoul & Tassoul (1996); Zahn (2013)) that is capable of explaining a possible spin-down from critical rotation to the presently observed super-synchronous values in binaries with such large periods.

A detailed set of massive star binary evolution models, including RLOF angular momentum transfer and tidal braking by oblate stellar models, against which to compare our results, is lacking in the literature. Detailed models and population synthesis simulations confronting the observa-

tions reported here will be published in a separate paper (Vanbeveren et al. 2016).

5 CONCLUSIONS

WR + O binaries may be progenitors of ultra-luminous supernovae, long-duration gamma-ray bursts and BH-BH mergers. Theory predicts that the O stars in WR + O binaries must have accreted significant amounts of angular momentum during RLOF from their companions. Only two O stars in WR+O binaries have previously published, measured values of $v_e \sin i$, and one other has a rough estimate. We report new $v_e \sin i$ measurements for 8 O stars in WR + O binaries. Using the literature values of i we then find the average equatorial rotational value of 348 km/s for 6 O stars, ranging from 237 to 482 km/s, from HeI lines. These values are highly super-synchronous. The observed super-synchronicity is in qualitative agreement with the predictions of short period, massive binary evolution models which include angular momentum transfer during RLOF and tidal braking afterwards. However, the super-synchronous nature of the two longest period binaries is a challenge to current tidal braking theory. We also find that the rotation rates of O stars in WR + O binaries, measured from HeI lines, are on average twice as large as those measured from HeII lines. We conclude that we are observing gravity darkening in these O stars, and predict that they are oblate.

ACKNOWLEDGMENTS

All of the new observations reported in this paper were obtained with the High Resolution Spectrograph (HRS) of the Southern African Large Telescope (SALT). We gratefully acknowledge the fine support of the astronomers and operators at the SALT Observatory. The generosity of the late Paul Newman and the Newman Foundation has made AMNH's participation in SALT possible; MMS gratefully acknowledges that support. S.M.C. acknowledges the South African Astronomical Observatory and the National Research Foundation of South Africa for support during this

² A case B binary has an initial orbital period such that RLOF starts while the mass loser is hydrogen-shell burning, i.e. prior to core helium burning. The periods of such binaries range between about 10 days and 1000 days.

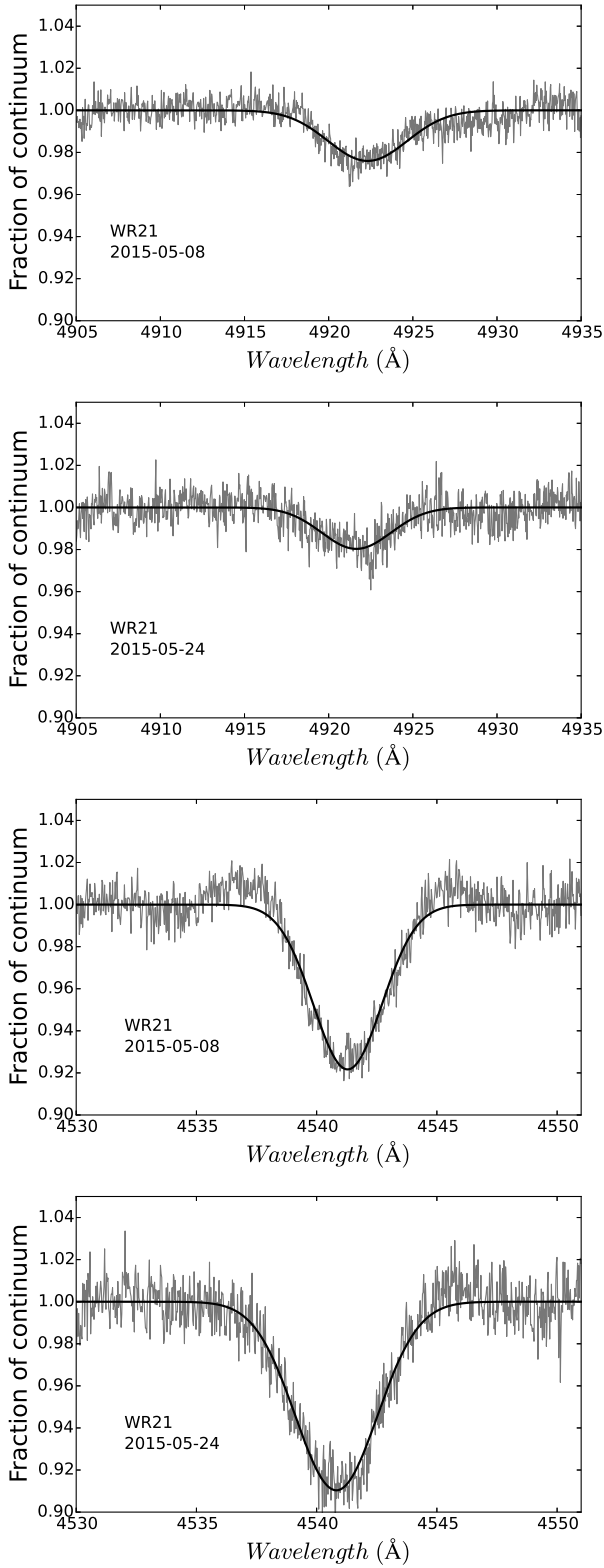


Figure 3. (Top) The HeI 4922 absorption line of WR 21 on 08 May 2015. (Second from Top) Same as above but on 24 May 2015. (Third from Top) The HeII 4541 absorption line of WR 21 on 08 May 2015. (Bottom) The HeII 4541 absorption line of WR 21 on 24 May 2015

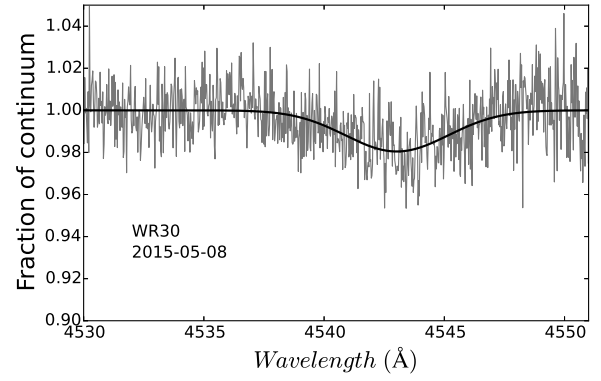


Figure 4. The HeII 4541 absorption line of WR 30 on 08 May 2015.

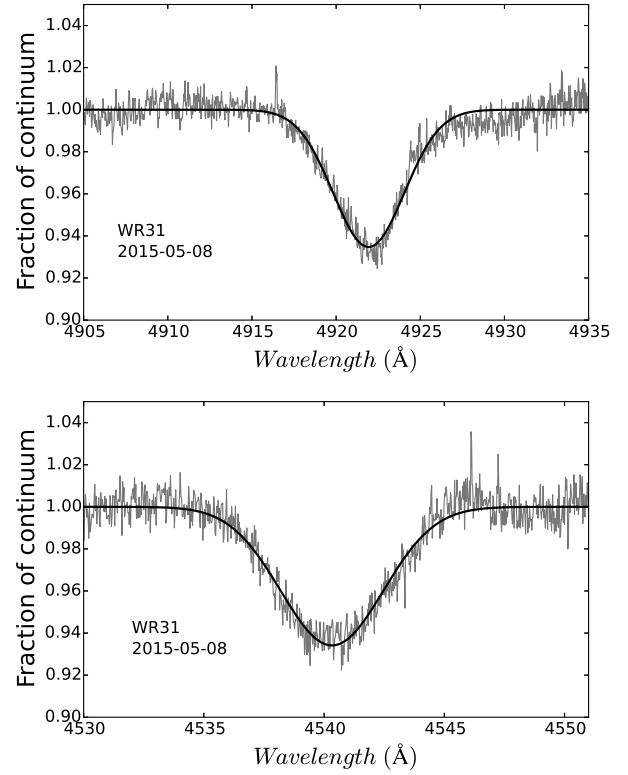


Figure 5. (Top) The HeI 4922 absorption line of WR 31 on 08 May 2015. (Bottom) The HeII 4541 absorption line of WR 31 on 08 May 2015.

project. We thank Ray Sharples and the Durham University team for construction and delivery of an excellent High Resolution Spectrograph. This research made use of Astropy, a community-developed core Python package for Astronomy (Astropy Collaboration, 2013). We thank Nibert Langer and Yong Shao for helpful suggestions. We also thank Professor Ian Howarth for two careful and thoughtful referee's reports, which resulted in significant improvements to the paper.

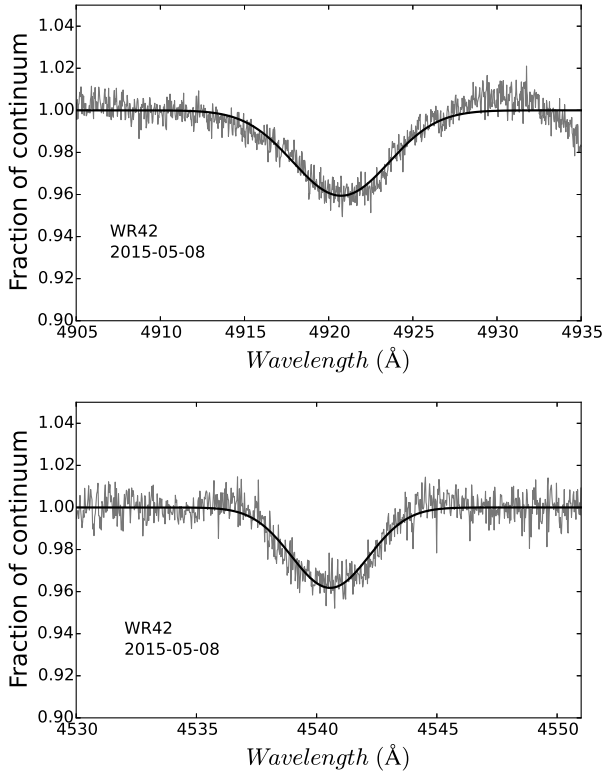


Figure 6. (Top) The HeI 4922 absorption line of WR 42 on 08 May 2015. (Bottom) The HeII 4541 absorption line of WR 42 on 08 May 2015.

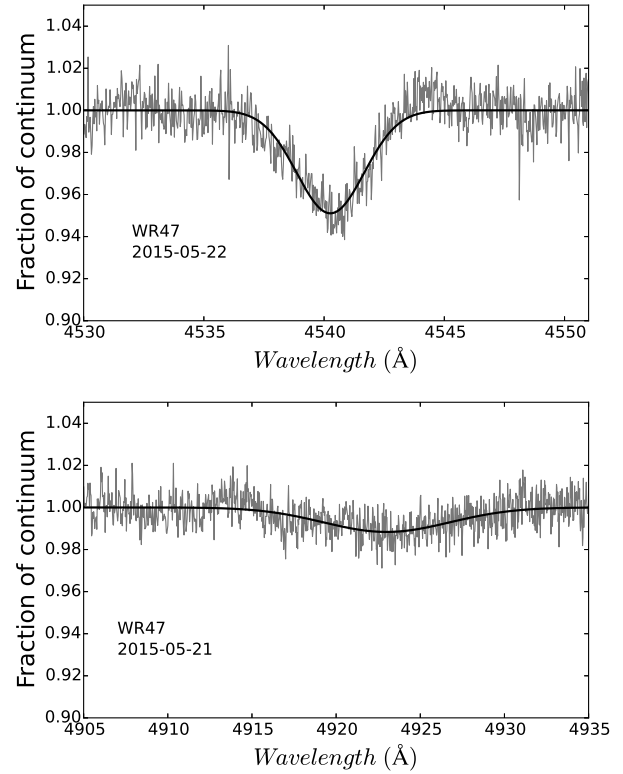


Figure 7. (Top) The HeII 4541 absorption line of WR 47 on 22 May 2015. (Bottom) The HeI 4922 absorption line of WR 47 on 21 May 2015.

REFERENCES

- Abbott B. P., et al., 2016, *PhRvL*, 116, 241102
 Astropy Collaboration, et al., 2013, *A&A*, 558, A33
 Baade D., Schmutz W., van Kerkwijk M., 1990, *A&A*, 240, 105
 Blaauw A., 1961, *BAN*, 15, 265
 Brott I., et al., 2011, *A&A*, 530, A116
 Claret A., 2016, *A&A*, 588, A15
 Craig M. W., et al., 2015, *ascl.soft*, ascl:1510.007
 Crause L. A., et al., 2014, *SPIE*, 9147, 91476T
 Crawford, S. M., Still, M., Schellart, P., et al., 2010, *SPIE*, 7737, 773725
 Crawford, S. M., and Craig, M. 2015, *Astrophysics Source Code Library*, submitted.
 Crawford, S. M., 2015, *Astrophysics Source Code Library*, submitted.
 Crowther P. A., 2015, *arXiv*, arXiv:1509.00495
 de La Chevrotière A., Moffat A. F. J., Chené A.-N., 2011, *MNRAS*, 411, 635
 de Mink S. E., Langer N., Izzard R. G., Sana H., de Koter A., 2013, *ApJ*, 764, 166
 Domiciano de Souza A., et al., 2014, *A&A*, 569, A10
 Dufton P. L., et al., 2013, *A&A*, 550, A109
 Espinosa Lara F., Rieutord M., 2011, *A&A*, 533, A43
 Ekström S., et al., 2012, *A&A*, 537, A146
 Georgy C., Meynet G., Walder R., Folini D., Maeder A., 2009, *A&A*, 502, 611
 Heger A., Langer N., 2000, *ApJ*, 544, 1016

- Hirschi R., Meynet G., Maeder A., 2004, *A&A*, 425, 649
 Howarth I. D., Siebert K. W., Hussain G. A. J., Prinja R. K., 1997, *MNRAS*, 284, 265
 Hut P., 1981, *A&A*, 99, 126
 Kushnir D., Zaldarriaga M., Kollmeier J. A., Waldman R., 2016, *MNRAS*, 462, 844
 Lamontagne R., Moffat A. F. J., Drissen L., Robert C., Matthews J. M., 1996, *AJ*, 112, 2227
 Maeder A., Meynet G., 2000, *A&A*, 361, 159
 Maíz Apellániz J., Alfaro E. J., Sota A., 2008, *arXiv*, arXiv:0804.2553
 Marchenko S. V., Moffat A. F. J., Koenigsberger G., 1994, *ApJ*, 422, 810
 Martins F., Schaerer D., Hillier D. J., 2005, *A&A*, 436, 1049
 Mason B. D., Gies D. R., Hartkopf W. I., Bagnuolo W. G., Jr., ten Brummelaar T., McAlister H. A., 1998, *AJ*, 115, 821
 Mason B. D., Hartkopf W. I., Gies D. R., Henry T. J., Helsel J. W., 2009, *AJ*, 137, 3358
 Massey P., 1981, *ApJ*, 244, 157
 McAlister H. A., et al., 2005, *ApJ*, 628, 43
 Moffat A. F. J., 2008, *IAUS*, 250, 119
 Monnier J. D., et al., 2007, *Sci*, 317, 342
 Nieva M.-F., Przybilla N., 2012, *A&A*, 539, A143
 Packet W., 1981, *A&A*, 102, 17
 Penny L. R., 1996, *ApJ*, 463, 737
 Petrovic J., Langer N., van der Hucht K. A., 2005, *A&A*, 435, 1013
 Pürrier M., Hannam M., Ohme F., 2016, *PhRvD*, 93, 084042
 Ramírez-Agudelo O. H., et al., 2013, *A&A*, 560, A29

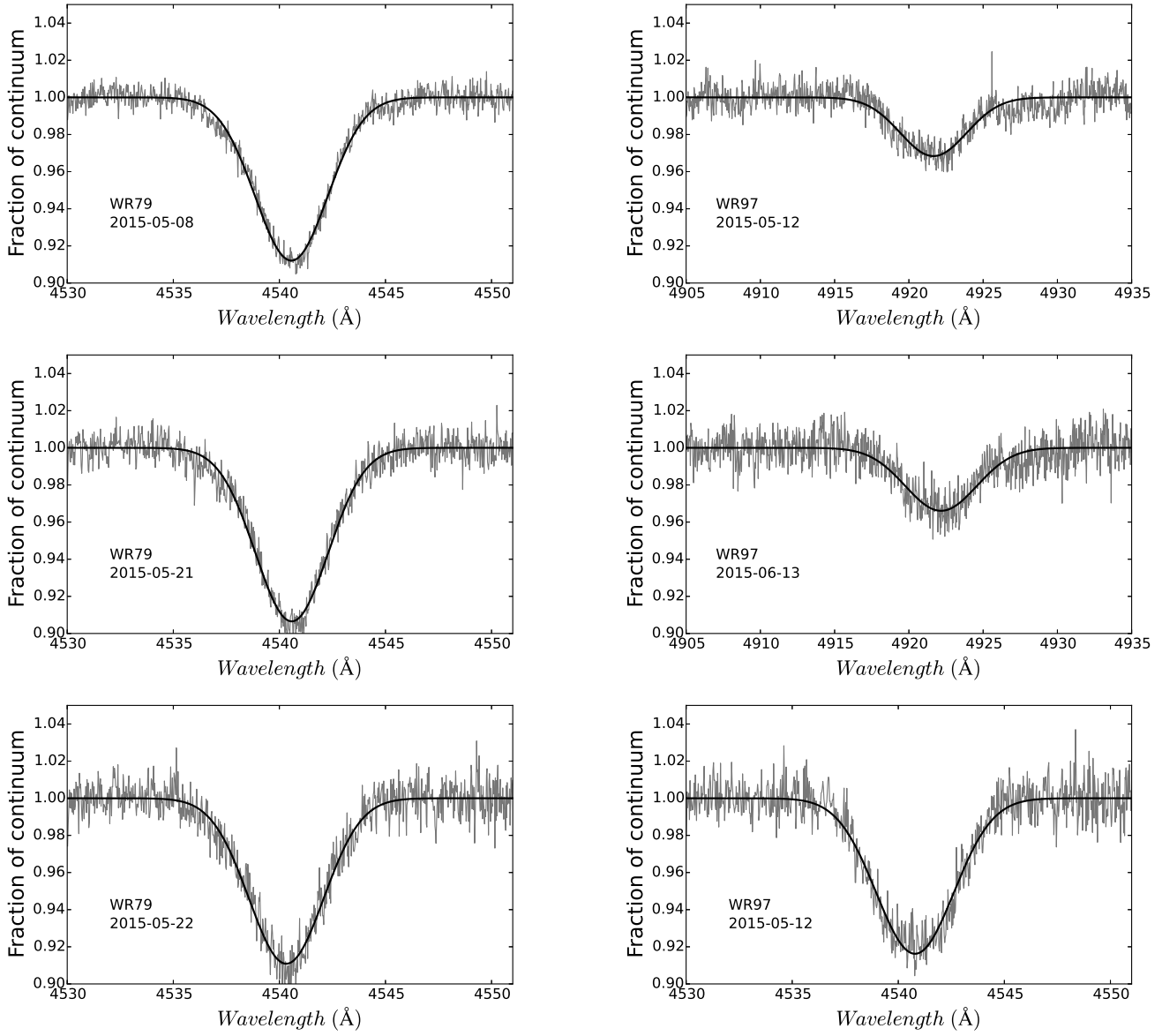


Figure 8. (Top) The HeII 4541 absorption line of WR 79 on 08 May 2015. (Middle) Same as above but on 21 May 2015. (Bottom) Same as above but on 22 May 2015.

- Ramírez-Agudelo O. H., et al., 2015, A&A, 580, A92
 Sana H., Evans C. J., 2011, IAUS, 272, 474
 Sana H., et al., 2013, A&A, 550, A107
 Schilbach E., Röser S., 2008, A&A, 489, 105
 Shara M. M., Faherty J. K., Zurek D., Moffat A. F. J., Gerke J., Doyon R., Artigau E., Drissen L., 2012, AJ, 143, 149
 Sota A., Maíz Apellániz J., Morrell N. I., Barbá R. H., Walborn N. R., Gamen R. C., Arias J. I., Alfaro E. J., 2014, ApJS, 211, 10
 Sundqvist J. O., Simón-Díaz S., Puls J., Markova N., 2013, A&A, 559, L10
 Tassoul J.-L., Tassoul M., 1996, FCPh, 16, 337
 van den Heuvel E. P. J., 1993, SSRv, 66, 309
 Vanbeveren D., De Loore C., Van Rensbergen W., 1998, A&ARv, 9, 63

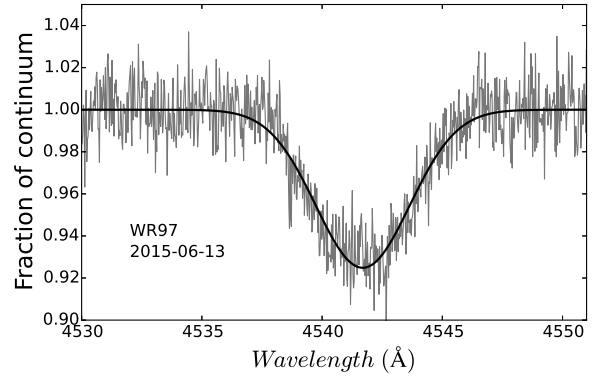


Figure 9. (Top) The HeI 4922 absorption line of WR 97 on 12 May 2015. (Second from Top) Same as above but on 13 June 2015. (Third from Top) The HeII 4541 absorption line of WR 97 on 12 May 2015. (Bottom) The HeII 4541 absorption line of WR 97 on 13 June 2015.

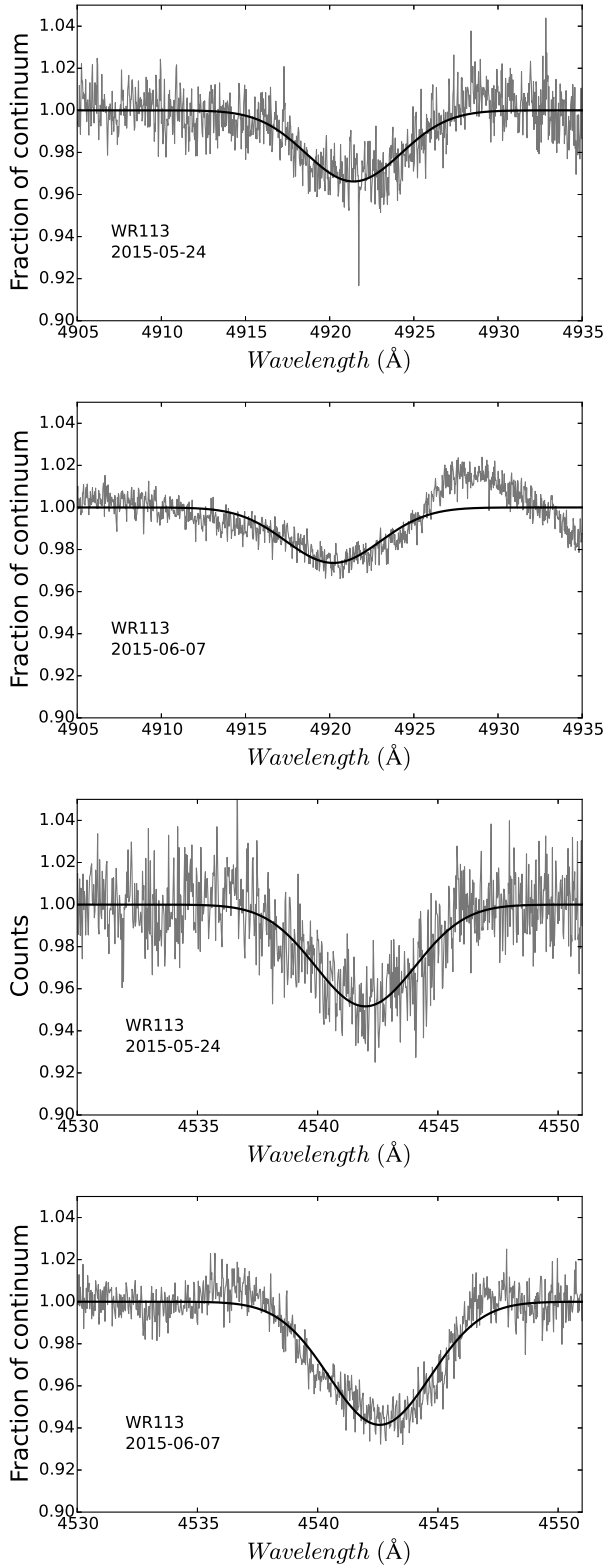


Figure 10. (Top) The HeI 4922 absorption line of WR 113 on 24 May 2015. (Second from Top) Same as above but on 07 June 2015. (Third from Top) The HeII 4541 absorption line of WR 113 on 24 May 2015. (Bottom) The HeII 4541 absorption line of WR 113 on 07 June 2015.

- Vanbeveren D., De Donder E., Van Bever J., Van Rensbergen W., De Loore C., 1998, *NewA*, 3, 443
 Vanbeveren D., Van Rensbergen, W., De Loore, C., 1998, *The Brightest Binaries*. Boston: Kluwer
 Vanbeveren D., 2009, *NewAR*, 53, 27
 Vanbeveren D., 2010, *ASPC*, 435, 115
 Vanbeveren D., 2010, *AIPC*, 1314, 361
 Vanbeveren D., 2010, *IAUS*, 266, 293
 Vanbeveren D., 2011, *BSRSL*, 80, 530
 Vanbeveren D., 2012, *ASPC*, 465, 342
 Vanbeveren D., Mennekens, N., Shara, M., Crawford, S., Moffat, A.F.J., Zurek, D., Crause, L., 2016, in preparation
 Villar-Sbaffi A., St-Louis N., Moffat A. F. J., Piirola V., 2005, *ApJ*, 623, 1092
 Villar-Sbaffi A., St-Louis N., Moffat A. F. J., Piirola V., 2006, *ApJ*, 640, 995
 von Zeipel H., 1924, *MNRAS*, 84, 665
 Woosley S. E., Heger A., 2006, *ApJ*, 637, 914
 Yoon S.-C., Langer N., 2005, *A&A*, 443, 643
 Zahn J.-P., 2013, *LNP*, 861, 301